Integrating Electrospun Microfibers into 3D Printed Scaffolds for Nerve Regeneration

Se-Jun Lee[1] , Wei Zhu[1] and Lijie Grace Zhang[1, 2, 3]

1. Department of Mechanical and Aerospace Engineering, The George Washington University 2. Department of Medicine, 3. Department of Biomedical Engineering, The George Washington University

THE GEORGE WASHINGTON UNIVERSITY
WASHINGTON, DC

School of Engineering & Applied Science
THE GEORGE WASHINGTON UNIVERSITY

INTRODUCTION

Electrospinning is a versatile technique to fabricate nano/microfibers for tissue engineering applications. In regard to neural regeneration, highly aligned, fibrous electrospun scaffolds can serve as excellent substrates, directing neural cells to elongate along the fibers. However, the electrospinning techniques often offer limited control over the constructive geometry and porosity. To date, one promising alternative is to combine the electrospinning technique and the emerging 3D bioprinting system in an effort to fabricate a novel tissue scaffold with both highly aligned and well-designed micro architecture. In this study, we introduced electrospun fibers into 3D printed microporous tissue constructs, and investigated neural stem cell (NSC) and primary neuronal cell growth in the neural tissue construct for the first time. The primary objectives of the present study are to (1) evaluate the feasibility of integrating electrospinning and stereolithography (SL) 3D printing to create a highly aligned and porous scaffold, and to (2) examine the proliferative capability and differentiation potential of NSCs and primary cortical neurons seeded in the resultant composite scaffold *in vitro*.

MATERIALS AND METHODS

Aligned polycaprolacton (PCL) and PCL/gelatin (50:50) microfibrous scaffolds were fabricated via our lab's electrospinning set-up. Prepared electrospun fibers were then placed on the bottom of petri dish followed by adding printable hydrogel inks (60 wt% – polyethylene (glycol) diacrylate (PEG-DA), 40 wt% PEG and photo initiator). SL printed scaffolds were designed as square pattern with 56% porosity using computer-aided design software. NSCs (ATCC) and primary cortical neurons were further seeded onto prewetted scaffolds and evaluated for cell adhesion and proliferation study.

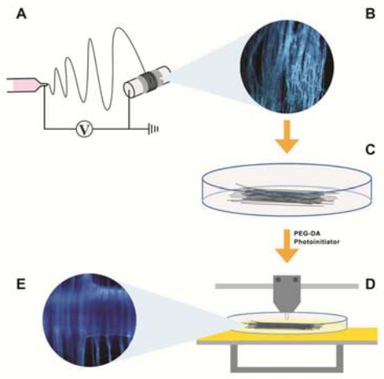

Figure 1. Schematic diagram of our 3D printed neural scaffold fabrication. (A) Our electrospinning set-up; (B) highly aligned electrospun fibers; (C) the PEG-DA suspension with aligned fibers in a petri dish; (D) SL printing scaffold; and (E) formation of a 3D neural scaffold embedded with electrospun fibers.

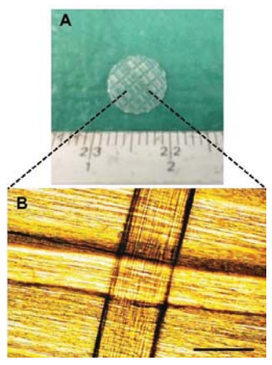

Figure 2. (A) Photo image of the 3D printed scaffold embedded with electrospun PCL fibers. (B) Microscopic view of the 3D printed scaffold with a highly aligned electrospun PCL fibers. Scale bar = 200 μm.

Scaffold Characterization

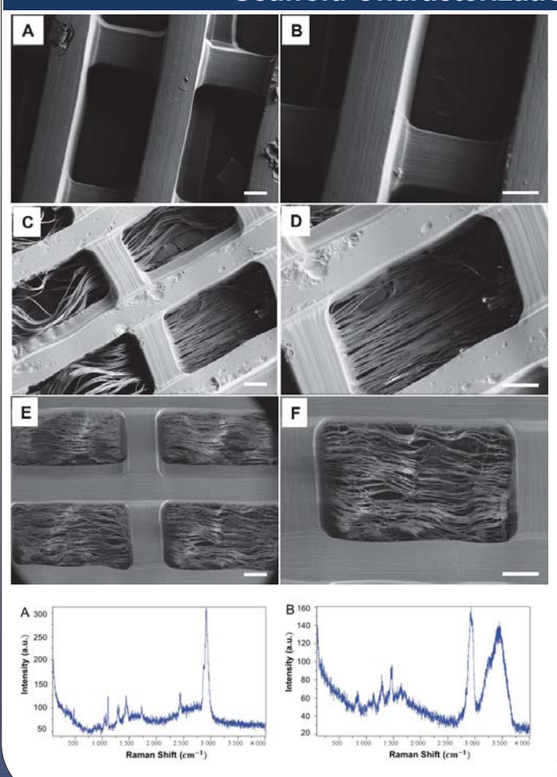

Figure 3. SEM images of 3D printed scaffolds with large porosity percentage of 66% (A and B); with PCL electrospun fibers (C and D); and PCL/gelatin electrospun fibers (E and F). A, C and E are at low magnification. B, D and F are at high magnification. Scale bar = 200 μm.

Figure 4. Raman spectroscopy of (A) the PEG-DA scaffold with PCL electrospun fibers and (B) the PEG-DA scaffold with PCL/gelatin electrospun fibers.

Samples	Young's modulus (MPa)	Ultimate tensile strength (MPa)
Control scaffold	0.35 ± 0.06	0.18 ± 0.02
Scaffolds with PCL fibers	2.31 ± 0.29*	0.93 ± 0.6*
Scaffolds with PCL/gelatin fibers	0.73 ± 0.21	0.51 ± 0.12

Table 1. Tensile testing of various scaffolds using the mechanical test system (MTS Criterion Model 42). Data are mean ± standard error of the mean; n=4. *p<0.05 when compared to all other scaffolds.

Samples	Contact Angle (°)
Control scaffold	36.8 ± 5.1
Scaffold with PCL fibers	48.1 ± 8.1
Scaffold with PCL/gelatin fibers	24.2 ± 9.7

Table 2. Surface wettability of scaffolds using a contact angle analyzer (DSA4 Kruss). Data are mean ± standard error of the mean; n=4.

NSC Proliferation and Differentiation

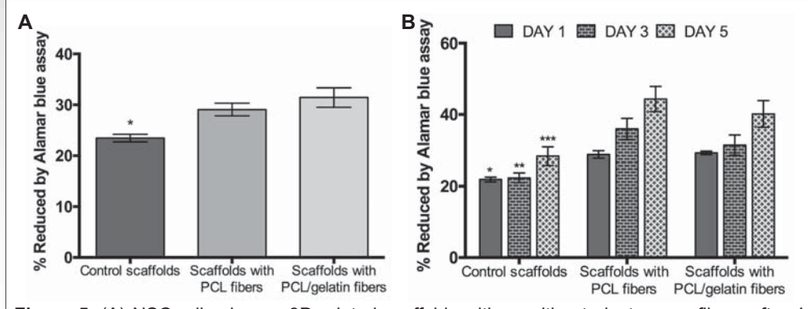

Figure 5. (A) NSC adhesion on 3D printed scaffolds with or without electrospun fibers after 4 hours of culture. Data are mean ± standard error of the mean; n=9. *p<0.05 when compared to all other scaffolds. (B) Enhanced NSC proliferation in 3D printed scaffolds with or without electrospun fibers after 5 day culture. Data are mean ± standard error of the mean, n=9; *p<0.05, **p<0.05 and ***p<0.05 when compared to all other scaffolds at day 1, 3 and 5 respectively.

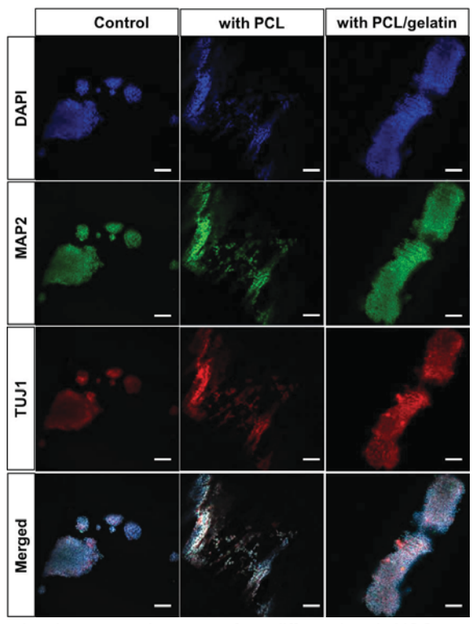

Figure 6. Confocal microscopy images of undifferentiated NSC growth and alignment morphology on scaffolds with or without electrospun fibers after 3 days of culture. Cell nuclei were stained by DAPI. Double staining of MAP2 and TUJ1 were used to detect neurite outgrowth of NSCs on various scaffolds. Scale bar = 100 μm.

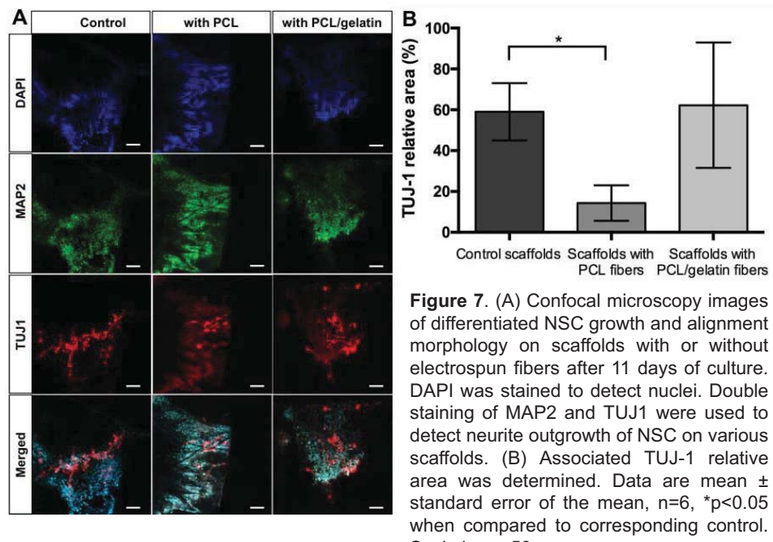

Figure 7. (A) Confocal microscopy images of differentiated NSC growth and alignment morphology on scaffolds with or without electrospun fibers after 11 days of culture. DAPI was stained to detect nuclei. Double staining of MAP2 and TUJ1 were used to detect neurite outgrowth of NSC on various scaffolds. (B) Associated TUJ-1 relative area was determined. Data are mean ± standard error of the mean, n=6, *p<0.05 when compared to corresponding control. Scale bar = 50 μm.

Primary cortical neuron outgrowth

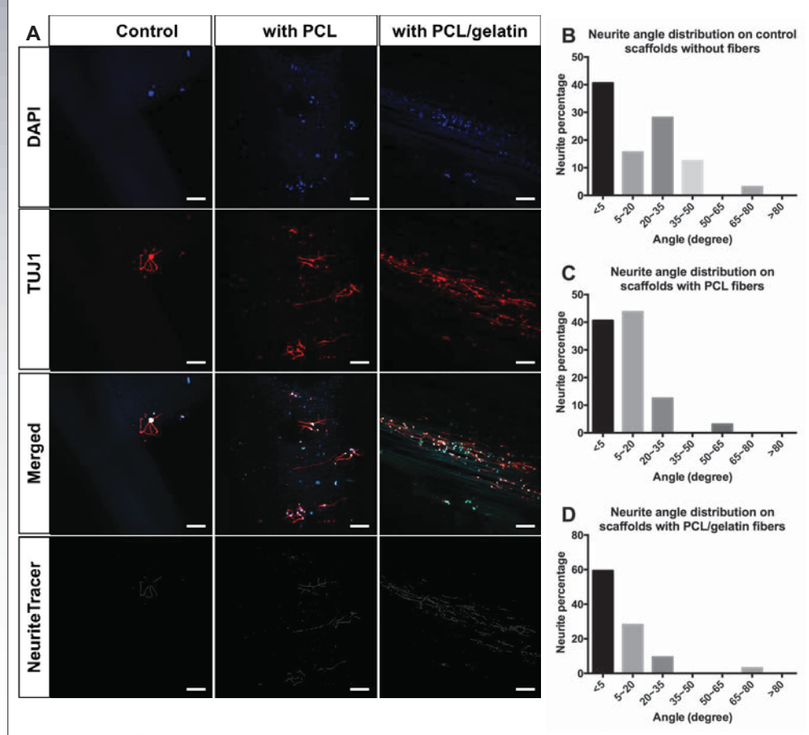

Figure 8. (A) Confocal microscopy images of neurite growth of primary cortical neurons on various 3D printed scaffolds with or without electrospun fibers at day 7. DAPI was stained to detect nuclei. TuJ1 was stained to detect neurite outgrowth of primary cells on various scaffolds after 7 days of culture. (B-D) The associated neurite outgrowth was traced automatically by NeuriteTracer. Scale bar = 100 μm. Neurite angle distributions on (B) control scaffolds without fibers, (C) scaffolds with PCL fibers and (D) scaffolds with PCL/gelatin fibers. N=6.

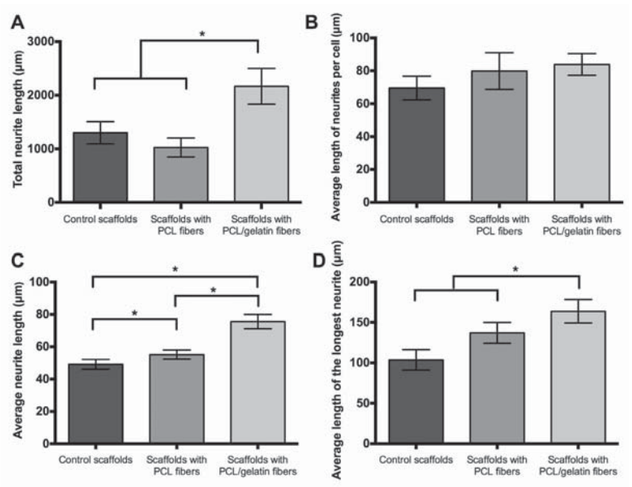

Figure 9. Quantification of neurite length of primary cortical neurons on 3D printed scaffolds with or without electrospun fibers after 7 days of culture. Neurite length was analyzed using ImageJ software and NeuriteTracer. (A) Total neurite length. (B) Average total length of neurites per cell. (C) Average neurite length, which is measured as the total neurite length divided by total neurite count. (D) Average length of the longest neurite per cell. Data are mean ± standard error of the mean, n=6, *p<0.05 when compared to corresponding groups at day 7.

CONCLUSION

This study demonstrated a novel approach for creating neural scaffold using a combination of SL 3D printing and electrospinning techniques. The resultant scaffold exhibited 3D printed microporous channels embedded with PCL or PCL/gelatin electrospun fibers. The incorporation of electrospun fibers into the 3D constructs result in enhanced mechanical properties. In addition, it was found that 3D printed scaffolds with PCL/gelatin fibers enhanced the neural stem cell differentiation compared to scaffolds with PCL alone fibers. Furthermore, a highly aligned PCL/gelatin fibers within the 3D printed scaffold improved the neurite outgrowth and directional control of primary cortical neurons.

ACKNOWLEDGEMENT

We would like to thank March of Dimes Foundation's Gene Discovery and Translational Research Grant for financial support.